Fully non-linear simulation of second-order resonance in a three-dimensional tank using the PSME method

AUTHOR QUERY FORM

ELSEVIER	**Journal:** APOR **Article Number:** 820	**Please e-mail or fax your responses and any corrections to:** **E-mail:** corrections.esch@elsevier.thomsondigital.com **Fax:** +353 6170 9272

Dear Author,

Please check your proof carefully and mark all corrections at the appropriate place in the proof (e.g., by using on-screen annotation in the PDF file) or compile them in a separate list. Note: if you opt to annotate the file with software other than Adobe Reader then please also highlight the appropriate place in the PDF file. To ensure fast publication of your paper please return your corrections within 48 hours.

For correction or revision of any artwork, please consult http://www.elsevier.com/artworkinstructions.

Any queries or remarks that have arisen during the processing of your manuscript are listed below and highlighted by flags in the proof. Click on the 'Q' link to go to the location in the proof.

Location in article	Query / Remark: click on the Q link to go Please insert your reply or correction at the corresponding line in the proof
Q1	Please confirm that given names and surnames have been identified correctly.
Q2	Please check the address for the corresponding author that has been added here, and correct if necessary.
Q3	Please update reference [19].
Q4	Please check the edit made in the caption of 'Fig. 19', and correct if necessary.

Thank you for your assistance.

Applied Ocean Research xx (2012) xxx–xxx

Contents lists available at SciVerse ScienceDirect

Applied Ocean Research

journal homepage: www.elsevier.com/locate/apor

Highlights

Applied Ocean Research xx (2012) xxx–xxx

Fully non-linear simulation of second-order resonance in a three-dimensional tank using the PSME method

Ming-Jyh Chern, Nima Vaziri*, Alistair G.L. Borthwick

► Non-linear second-order sloshing waves in a three-dimensional shallow water tank are simulated using a PSME method. ► The effects of excitation frequency, water depth, base ratio and amplitude of excitation are studied. ► The wave pattern is highly dependent on the water depth in the tank, but relatively insensitive to excitation amplitude. ► The non-linearity effects are significant in the second-order sloshing in shallow water.

Applied Ocean Research xxx (2012) xxx–xxx

Contents lists available at SciVerse ScienceDirect

Applied Ocean Research

journal homepage: www.elsevier.com/locate/apor

Fully non-linear simulation of second-order resonance in a three-dimensional tank using the PSME method

Q1 Ming-Jyh Chern[a,b], Nima Vaziri[a,c,*], Alistair G.L. Borthwick[d]

[a] Department of Mechanical Engineering, National Taiwan University of Science and Technology, 43 Sec. 4 Keelung Road, Taipei 10607, Taiwan
[b] Ecological Engineering Research Unit, National Taiwan University, No. 1 Sec. 4 Roosevelt Road, Taipei 10617, Taiwan
[c] Department of Physics, Karaj Branch, Islamic Azad University, Karaj, Iran
[d] Department of Civil and Environmental Engineering, University Collage Cork, Cork, Ireland

ARTICLE INFO

Article history:
Received 9 December 2011
Received in revised form 21 February 2012
Accepted 25 February 2012
Available online xxx

Keywords:
Second-order resonance
PSME method
Three-dimensional tank
Shallow water

ABSTRACT

Sloshing occurs when a partially filled tank is subject to external excitation. If the excitation frequency is equal to half of the second-order natural frequency obtained from the linear theory, then second-order resonance may occur. But it gradually modifies to standing waves. Moreover, violent second-order resonant free surface motions may be induced when the sum (or difference) of the excitation frequency and any one of the natural frequencies is equal to another natural frequency. In this study, fully non-linear second-order resonance waves in a three-dimensional shallow water rectangular tank are simulated using a pseudospectral σ-transformation model. The model is validated against results from three benchmark tests for which there are published analytical and numerical solutions available. A detailed analysis is presented of sloshing in a shallow water tank, with the main excitation and response frequencies identified from the power spectra. Large amplitude free surface motions are observed whenever second-order resonance occurs. In certain cases, the wave pattern in the tank is different to that predicted from linear analysis of second-order resonance, due to the effect of nonlinearity. Results are presented from a parameter study examining the influences of water depth, base aspect ratio, and excitation amplitude on the wave motions and patterns. It is found that the wave pattern is highly dependent on the water depth in the tank, but relatively insensitive to excitation amplitude. Also, the decay patterns are seen when the second-order resonance excitations are applied vertically. The study demonstrates that second-order resonance can be very pronounced in shallow water.

1. Introduction

Any container that is partially filled with liquid can be susceptible to sloshing motions if the container is subjected to external forcing. Sloshing hazards can typically develop in liquid storage tanks where the forcing may be due to movement of the tank due to transport (i.e. by ship) or natural disturbance (e.g. earthquake). In cases where the frequency of the external forcing is close to one of the natural frequencies of motion of the liquid in the container, resonance free surface motions can then occur leading to greatly increased structural loading, which in turn may damage the tank walls. Ibrahim [1] and Faltinsen and Timokha [2] provide comprehensive reviews on the physics of liquid sloshing.

Many previous studies (see e.g. Faltinsen [3], Wu et al. [4] and Chern et al. [5]) focused on resonant sloshing at the first-order natural frequency. However, resonance may occur due to high order sub-harmonics. Wu [6] undertook a detailed second-order analysis of sloshing in a two-dimensional rectangular tank, and predicted that resonance would occur when the excitation frequency is equal to half the second-order (or any of the even modes) of the natural frequencies. Also, when the sum (or the difference) of an excitation frequency and any one of the natural frequencies is equal to another natural frequency, the motion might become violent. This theory has been confirmed by Wang and Wu [7] for the wave interactions with two bodies floating on the water surface. Wu's analysis is based on perturbation theory using a small parameter expansion, and so is not applicable at resonance, if the free surface motions become very violent. With this in mind, Wang et al. [8] used a high order finite element method to analyse the motion of liquid confined between two floating cylinders. Their study demonstrates that quantitative differences can develop between fully non-linear and linear simulations of second-order resonance, especially after a long period of time. Other relevant studies of two-dimensional sloshing are by Liu et al. [9] and Firouz-Abadi et al. [10].

Two-dimensional sloshing models are limited to planar wave motions in-line with or opposing the direction of excitation. At

Q2 * Corresponding author at: Department of Mechanical Engineering, National Taiwan University of Science and Technology, 43 Sec. 4 Keelung Road, Taipei 10607, Taiwan. Tel.: +886 2 2737 7315; fax: +886 2 2737 6460.
E-mail address: n.vaziri@gmail.com (N. Vaziri).

0141-1187/$ – see front matter © 2012 Elsevier Ltd. All rights reserved.
doi:10.1016/j.apor.2012.02.005

resonance, strongly three-dimensional free surface motions may arise, even leading to chaotic behavior (as discussed e.g. by Faltinsen et al. [11]). First-order sloshing in three-dimensions has been considered in a series of papers by Faltinsen et al. [11–13]. To the authors' knowledge, there is only one published study to date on higher order sloshing in three-dimensional tanks; this is by Faltinsen et al. [12] who focused on the higher modes of liquid sloshing in a tank with a square base.

The present paper describes a Chebyshev pseudospectral matrix-element (PSME) model (following Ku and Hatziavramidis [14], Chern et al. [5,15] and Vaziri et al. [16]) of the second-order resonant motions of an inviscid fluid in a three-dimensional rectangular tank. The flow physics is represented mathematically by fully non-linear potential flow theory in a σ-transformed coordinate system that maps the liquid domain onto a rectangle (and thus overcomes problems of specifying the free surface explicitly). A consequence of the mapping is that the free surface cannot be vertical, overturning, or breaking. Results are presented for second-order resonance in shallow water where the depth to length ratio, $d/a = 0.1$ (which is the border between intermediate water depth and shallow water depth [2]). This is in keeping with Wu [6] who observed that second-order resonance has a more significant effect for small values of d/a.

2. Mathematical model of free surface waves in the Cartesian domain

Fig. 1 illustrates the model domain, where a and b are the length and the width of the tank, respectively. The still water depth is denoted d. The physical domain is defined as $x, y, z \in [0, a] \times [0, b] \times [-d, \eta]$. In the discussion to follow, we will refer to six sampling locations where the free surface elevation time histories will be considered: the four corner points, A, B, C and D, and two middle wall locations, E and F. For an incompressible, inviscid, and irrotational fluid, we define the velocity potential φ, satisfying Laplace's equation, such that:

$$\frac{\partial^2\varphi}{\partial x^2} + \frac{\partial^2\varphi}{\partial y^2} + \frac{\partial^2\varphi}{\partial z^2} = 0, \tag{1}$$

For there to be no flow through the lateral walls and bed of the tank and therefore the normal velocity components are set to zero, we require:

$$\frac{\partial\varphi}{\partial x} = 0 \quad \text{at} \quad x = 0 \quad \text{and} \quad x = a, \tag{2}$$

$$\frac{\partial\varphi}{\partial y} = 0 \quad \text{at} \quad y = 0 \quad \text{and} \quad y = b, \tag{3}$$

and

$$\frac{\partial\varphi}{\partial z} = 0 \quad \text{at} \quad z = -d. \tag{4}$$

It means that the flow can slip but cannot penetrate to the wall. Let the excitation displacements of the tank be:

$$\begin{aligned} D_x &= A_x \sin(\omega_x t), \\ D_y &= A_y \sin(\omega_y t) \\ &\text{and} \\ D_z &= A_z \sin(\omega_z t) \end{aligned} \tag{5}$$

where A is an amplitude, t is time and ω is the excitation frequency, and the subscripts x, y and z refer to surge, sway and heave, respectively. By differentiating Eq. (5) twice with respect to time, we obtain the tank acceleration components, $(d^2D_x)/(dt^2)$, $(d^2D_y)/(dt^2)$ and $(d^2D_z)/(dt^2)$.

Using linear theory, the natural frequencies of sloshing in a rectangular tank may be expressed (see e.g. Faltinsen [3] and Wu et al. [4]):

$$\omega_{mn}^2 = g\pi\sqrt{\left(\frac{m^2}{a^2} + \frac{n^2}{b^2}\right)} \tan h\left(\pi\sqrt{\left(\frac{m^2}{a^2} + \frac{n^2}{b^2}\right)}d\right), \quad (m, n = 1, 2, \ldots), \tag{6}$$

in which g is the acceleration due to gravity. The non-linear dynamic free surface boundary condition is:

$$\frac{\partial\varphi}{\partial t} = \frac{\partial\varphi}{\partial z}\frac{\partial\eta}{\partial t} - g\eta - \frac{1}{2}\left[\left(\frac{\partial\varphi}{\partial x}\right)^2 + \left(\frac{\partial\varphi}{\partial y}\right)^2 + \left(\frac{\partial\varphi}{\partial z}\right)^2\right] - x\frac{d^2D_x}{dt^2} - y\frac{d^2D_y}{dt^2} - z\frac{d^2D_z}{dt^2} \quad \text{at} \quad z = \eta, \tag{7}$$

and the non-linear kinematic free surface boundary condition is:

$$\frac{\partial\eta}{\partial t} = \frac{\partial\varphi}{\partial z} - \frac{\partial\varphi}{\partial x}\frac{\partial\eta}{\partial x} - \frac{\partial\varphi}{\partial y}\frac{\partial\eta}{\partial y} \quad \text{at} \quad z = \eta, \tag{8}$$

where η is the free surface elevation above mean water level (see chapter three of Dean and Dalrymple [17] and Wu et al. [4] for more details). Initial values of the dependent variables φ and η are given by:

$$\varphi(x, y, z, 0) = -x\left.\frac{dD_x}{dt}\right|_{t=0} - y\left.\frac{dD_y}{dt}\right|_{t=0}, \tag{9}$$

and

$$\eta(x, y, 0) = 0. \tag{10}$$

2.1. σ-Transformation

Following Philips [18], a σ-transformation is used to convert the time-varying physical domain (due to the moving free surface) where $x, y, z \in [0, a] \times [0, b] \times [-d, \eta]$ to a fixed computational domain where $X, Y, \sigma \in [-1, 1] \times [-1, 1] \times [-1, 1]$. The governing equation and its boundary conditions are altered accordingly to apply on the stretched grid system. The above problem involves a pair of nonlinear free surface conditions, Eqs. (7) and (8), which are applied to a transient free surface elevation $\eta(x, t)$ at $t > 0$. Herein, this difficulty and also the moving free surface complication are handled by this method in the computational domain. The linear transformation is expressed as:

$$\begin{aligned} X &= -1 + \frac{2x}{a}, \\ Y &= -1 + \frac{2y}{b}, \\ \sigma &= -1 + \frac{2(z+d)}{h}, \end{aligned} \tag{11}$$

where

$$h = \eta + d. \tag{12}$$

Although this is a very simple transform to implement, it is restricted to a free surface which has unique liquid connectivity in the vertical to the bed. In order words, the transformation breaks down for any wave that has a vertical face, or is overturning, or is breaking. Similarly, it is unable to handle free surface motions that collide with the roof of the container.

The σ-transform maps the velocity potential from $\varphi(x, y, z, t)$ in the physical domain onto $\Phi(X, Y, \sigma, t)$ in the transformed domain. After applying the chain rule and rearranging, the transformed governing equation becomes:

Please cite this article in press as: Chern M-J, et al. Fully non-linear simulation of second-order resonance in a three-dimensional tank using the PSME method. Applied Ocean Research (2012), doi:10.1016/j.apor.2012.02.005

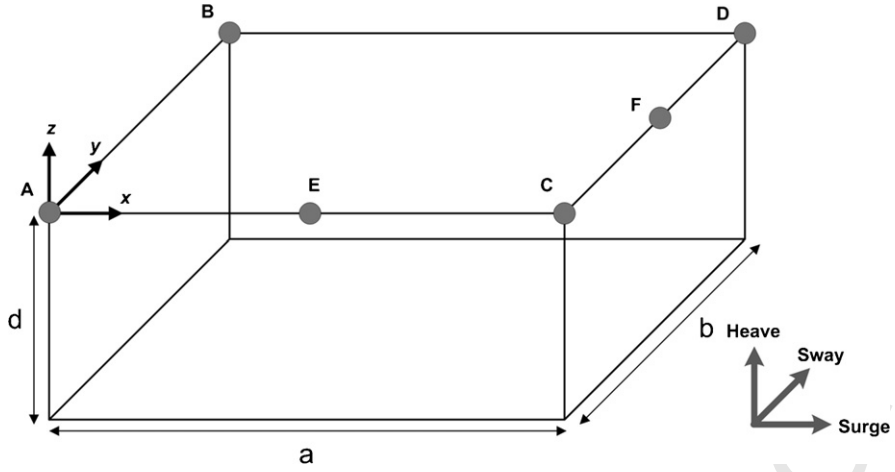

Fig. 1. Model tank and excitation (external forcing) directions.

$$\left(\frac{2}{a}\right)^2\frac{\partial^2\Phi}{\partial X^2}+\left(\frac{2}{b}\right)^2\frac{\partial^2\Phi}{\partial Y^2}+\left[\left(\frac{2}{a}\right)^2\left(\frac{2\sigma}{h^2}\right)\left(\frac{\partial\eta}{\partial X}\right)^2-\left(\frac{2}{a}\right)^2\left(\frac{\sigma}{h}\right)\left(\frac{\partial^2\eta}{\partial X^2}\right)\right.$$
$$\left.+\left(\frac{2}{b}\right)^2\left(\frac{2\sigma}{h^2}\right)\left(\frac{\partial\eta}{\partial Y}\right)^2-\left(\frac{2}{b}\right)^2\left(\frac{\sigma}{h}\right)\left(\frac{\partial^2\eta}{\partial Y^2}\right)\right]\frac{\partial\Phi}{\partial\sigma}$$
$$-\left[\left(\frac{2}{a}\right)^2\left(\frac{2\sigma}{h}\right)\left(\frac{\partial\eta}{\partial X}\right)\right]\frac{\partial^2\Phi}{\partial X\partial\sigma}-\left[\left(\frac{2}{b}\right)^2\left(\frac{2\sigma}{h}\right)\left(\frac{\partial\eta}{\partial Y}\right)\right]\frac{\partial^2\Phi}{\partial Y\partial\sigma}$$
$$+\left[\left(\frac{2}{a}\right)^2\left(\frac{\sigma^2}{h^2}\right)\left(\frac{\partial\eta}{\partial X}\right)^2+\left(\frac{2}{b}\right)^2\left(\frac{\sigma^2}{h^2}\right)\left(\frac{\partial\eta}{\partial Y}\right)^2+\left(\frac{1}{h^2}\right)\right]\frac{\partial^2\Phi}{\partial\sigma^2}=0. \quad (13)$$

The boundary conditions, Eqs. (2)–(4), (7) and (8), are transformed in a similar fashion (see e.g. Chern et al. [19]).

2.2. PSME modeling

The transformed governing equation and boundary conditions are discretised in the transformed domain using the Chebyshev collocation method where N, M and L are the total numbers of collocation points in the X, Y and σ directions. A typical physical grid system is depicted in Fig. 2. PSME discretisations are used to represent all spatial derivatives, such that $\frac{\partial\Phi}{\partial\sigma}=\sum_{m=0}^{L}\hat{\mathbf{G}}\boldsymbol{\sigma}^{(1)}_{km}\Phi_{ijm}$ and $\frac{\partial^2\Phi}{\partial X^2}=\sum_{m=0}^{N}\hat{\mathbf{G}}\mathbf{X}^{(2)}_{im}\Phi_{mjk}$ wherein $\hat{\mathbf{G}}\boldsymbol{\sigma}^{(1)}_{km}$ and $\hat{\mathbf{G}}\mathbf{X}^{(2)}_{im}$ are Chebyshev matrix coefficients in the σ and X directions. A third-order Adam–Bashforth (AB3) scheme is used for time integration. Full details of the discretised equations are given by Chern et al. [19].

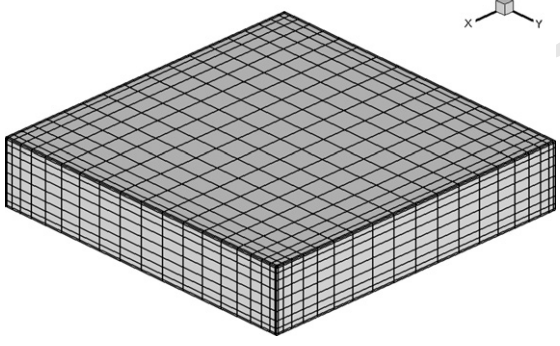

Fig. 2. Three-dimensional pseudospectral σ-transformed mesh.

The numerical solver is implemented as follows. First, an initial free surface profile is input. Then, free surface boundary values of Φ are determined from the pseudospectral σ-transformed version of Eq. (7). The pseudospectral σ-transformed governing equation is then solved iteratively using successive-over relaxation together with the bed and wall boundary conditions. The free surface elevation, η, is computed using the pseudospectral σ-transformed version of Eq. (8). The time is incremented one time step, and the process repeated successively until the simulation is complete.

3. Validation

A full description is given by Chern et al. [19] of the model validation for two near-resonant 2-D sloshing cases previously investigated by Faltinsen [3], Wu et al. [4], and Chern et al. [5] for surge excitation of water in a rectangular tank where $a/d=2.0$ and $b/d=0.2$. Chern et al. [19] also present further model validation for near-resonant 3-D sloshing in a square tank where the depth to length ratio is 0.25, and obtain results in close agreement with those of Wu et al. [4].

4. Second-order resonance in shallow water tank

Let us consider the longitudinal excitation of water in a tank of dimensions $a/d=b/d=10$ and the non-dimensional amplitude is $A_x/d=0.001$. Figs. 3–6 show the free surface elevation time histories and associated power spectra obtained at Point A for excitation frequencies equal to $0.9999\omega_{20}$, $\omega_{20}/2$, $\omega_{20}+\omega_{10}$ and $\omega_{20}-\omega_{10}$ (following Wu [6]) where ω_{10} and ω_{20} are the first-order and second-order natural frequencies in the x-direction, respectively (see Eq. (6)).

For $\omega_x=0.9999\omega_{20}$, the wave train is irregular and decays gradually (Fig. 3). Although the first natural frequency dominates, there is a significant contribution at the second harmonic, and lesser contributions at other harmonics. Resonance occurs when $\omega_x=\omega_{20}/2$ and $\omega_x=\omega_{20}-\omega_{10}$ (Figs. 4 and 6). The free surface oscillations increase monotonically in both cases, though the rate of increase in amplitude for an excitation frequency of $\omega_x=\omega_{20}/2$ is about 50% more than for $\omega_x=\omega_{20}-\omega_{10}$. In both cases, the

Please cite this article in press as: Chern M-J, et al. Fully non-linear simulation of second-order resonance in a three-dimensional tank using the PSME method. Applied Ocean Research (2012), doi:10.1016/j.apor.2012.02.005

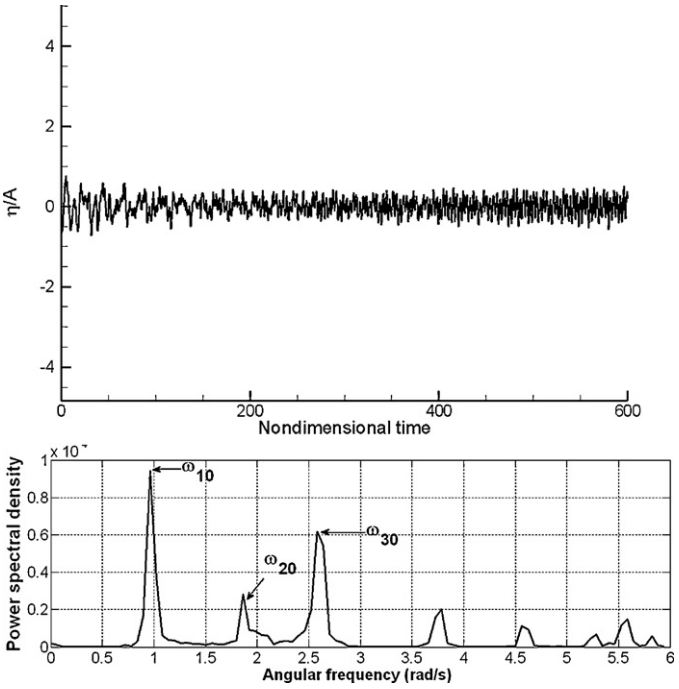

Fig. 3. Free surface time history and power spectrum at Point A for surge excitation frequency $\omega_x = 0.9999\omega_{20}$; the natural frequencies are $\omega_{10} = 0.9683$ rad/s, $\omega_{20} = 1.8527$ rad/s and $\omega_{30} = 2.6092$ rad/s.

resonance patterns gradually modify to high elevations standing waves. When the excitation frequency is equal to half of the second-order natural frequency, the free surface motions occur at the first natural frequency and the excitation frequency. In the case of the $\omega_x = \omega_{20} - \omega_{10}$, the dominant frequency is the excitation frequency. When the excitation frequency is $\omega_x = \omega_{20} + \omega_{10}$ the free surface motions exhibit a pronounced beating behavior

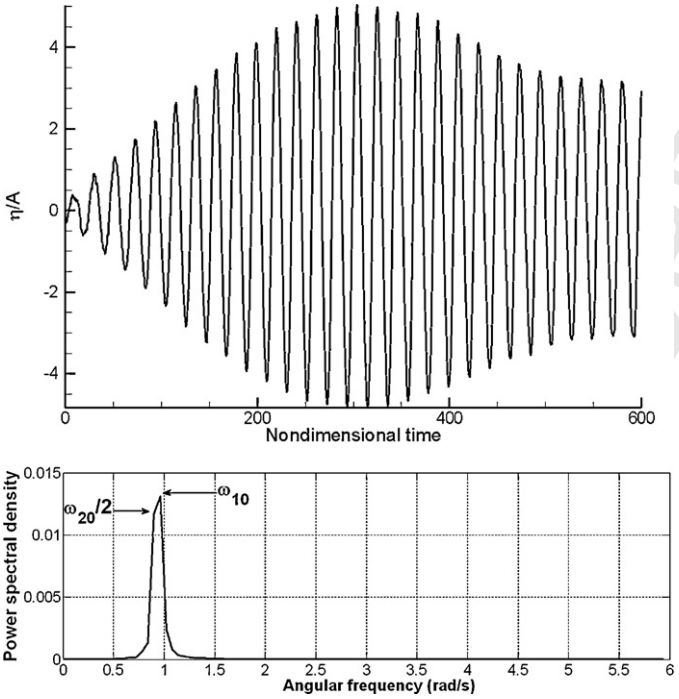

Fig. 4. Free surface time history and power spectrum at Point A for surge excitation frequency $\omega_x = \omega_{20}/2$; the natural frequencies are $\omega_{10} = 0.9683$ rad/s and $\omega_{20}/2 = 0.9264$ rad/s.

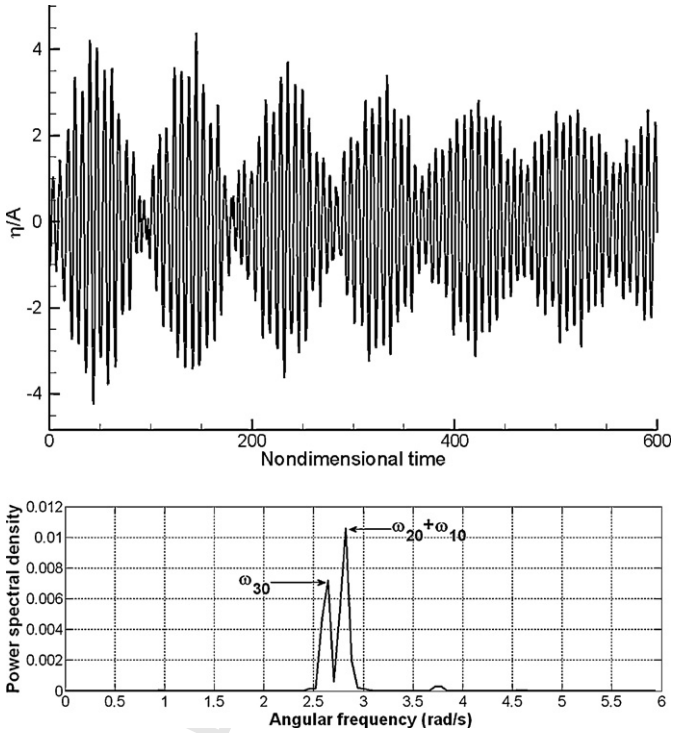

Fig. 5. Free surface time history and power spectrum at Point A for surge excitation frequency $\omega_x = \omega_{20} + \omega_{10}$; the natural frequency is $\omega_{30} = 2.6092$ rad/s and sum natural frequency is $\omega_{20} + \omega_{10} = 2.8210$ rad/s.

(Fig. 5) with an envelope period of about 95 non-dimensional time units. In this case, elevations of waves and also the difference between the maximum and minimum elevations in each beat gradually decrease. The beating pattern in the summation

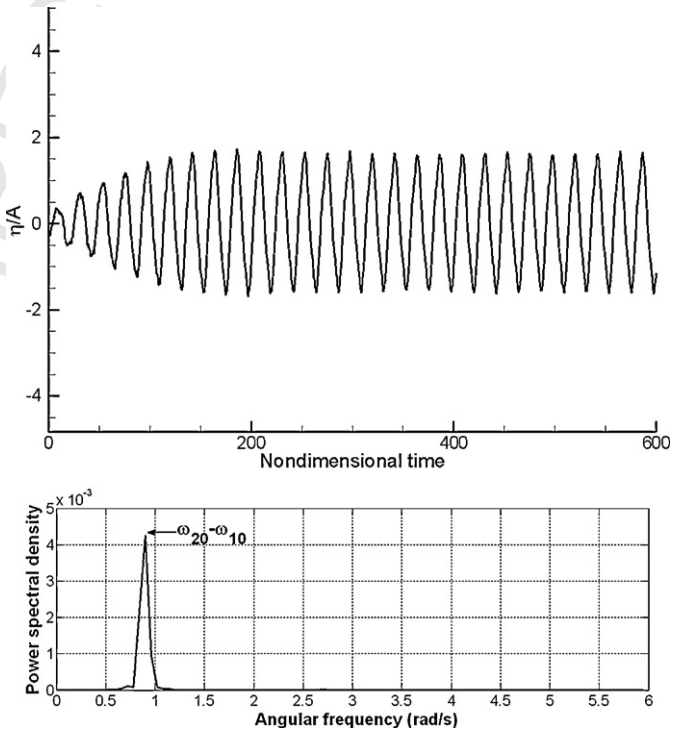

Fig. 6. Free surface time history and power spectrum at Point A for surge excitation frequency $\omega_x = \omega_{20} - \omega_{10}$; the difference natural frequency is $\omega_{20} - \omega_{10} = 0.8844$ rad/s.

Please cite this article in press as: Chern M-J, et al. Fully non-linear simulation of second-order resonance in a three-dimensional tank using the PSME method. Applied Ocean Research (2012), doi:10.1016/j.apor.2012.02.005

condition is due to the close proximity of the third-order natural frequency ω_{30} to the forcing excitation frequency. The results presented here, except for $\omega_x = \omega_{20} + \omega_{10}$, are generally consistent with the discussion by Wu [6]; the discrepancy is most likely to be due to the effect of non-linearity (as discussed by Wang et al. [8]). All cases (with $40 \times 40 \times 10$ grid points in x, y and z directions, respectively and 0.01 as a nondimensional time step, $\Delta t^* = \Delta t\sqrt{\left(\frac{g}{d}\right)}$) have been computed on a workstation with two Intel Xenon 3.10 GHz CPU processors and 6GB RAM memory. The CPU time required for all cases is less than 75 h. Previous studies have shown that the PSME method gives convergent and stable results for wide ranges of collocation point numbers and time step. Details of the stability and the mesh convergence in the three-dimensional sloshing problems can be found in Chern et al. [19].

These results confirm the importance of second-order resonance in shallow water tanks, which can induce major changes to the wave pattern and wave regime. To study the effect of second-order resonance on first-order resonance, the tank is excited in near-resonant surge at $\omega_x = 0.9999\omega_{10}$ of amplitude $A_x/d = 0.001$ with a second-order sway excitation at $\omega_y = \omega_{20}/2$ also of amplitude $A_y/d = 0.001$ applied simultaneously. Fig. 7 compares the free surface elevation time histories obtained for the surge excitation with and without the second-order sway excitation. Although the second-order excitation raises the maximum wave elevation at Point A by about 63%, the maximum wave elevation decreases at Point B about 38%. Phase shifting is evident. Without second-order sway excitation, resonance occurs and the wave regime is planar in surge, as expected (Fig. 8). When second-order excitation is added, resonance occurs but the wave regime is diagonal, comprising a standing wave oscillating from one corner to the opposite corner with much less motion in other corners (Fig. 9).

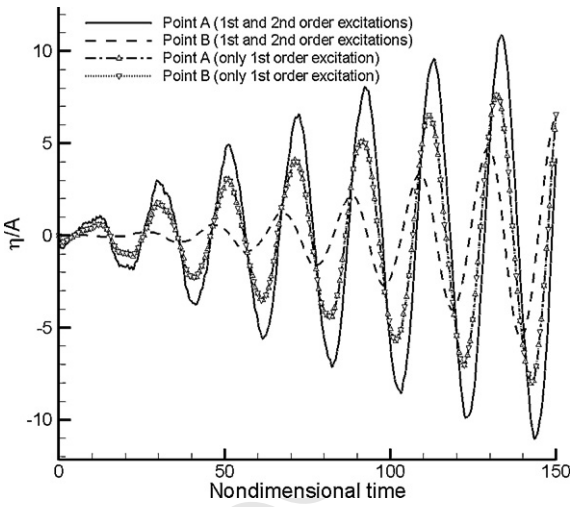

Fig. 7. Free surface elevation time histories for excitation amplitude: (i) near-resonant first-order $\omega_x = 0.9999\omega_{10}$, $A_x/d = 0.001$; and (ii) near-resonant first-order $\omega_x = 0.9999\omega_{10}$, $A_x/d = 0.001$, and second-order $\omega_y = \omega_{20}/2$, $A_y/d = 0.001$.

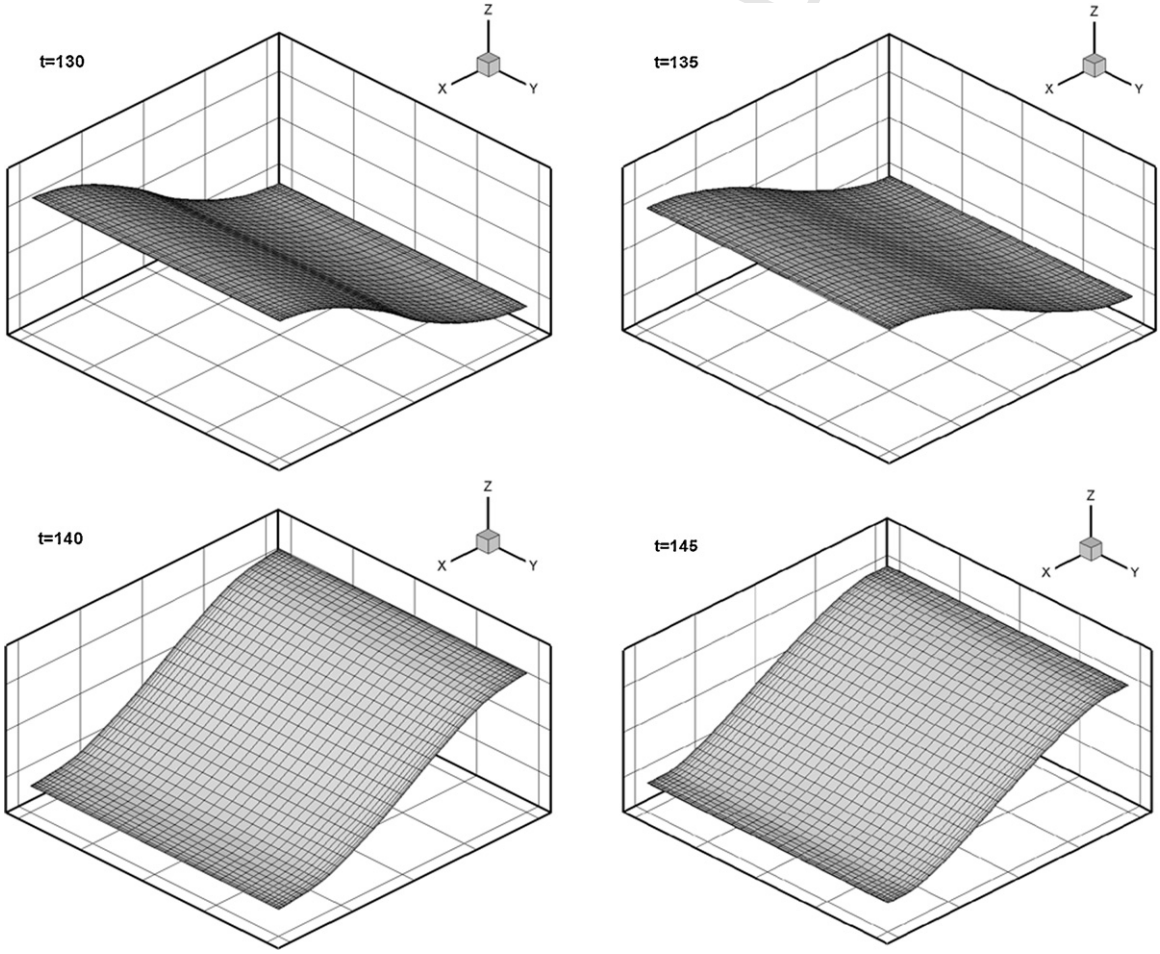

Fig. 8. 3-D visualisations (not to scale) of the liquid free surface sloshing: $A_x/d = 0.001$, $\omega_x = 0.9999\omega_{10}$.

Please cite this article in press as: Chern M-J, et al. Fully non-linear simulation of second-order resonance in a three-dimensional tank using the PSME method. Applied Ocean Research (2012), doi:10.1016/j.apor.2012.02.005

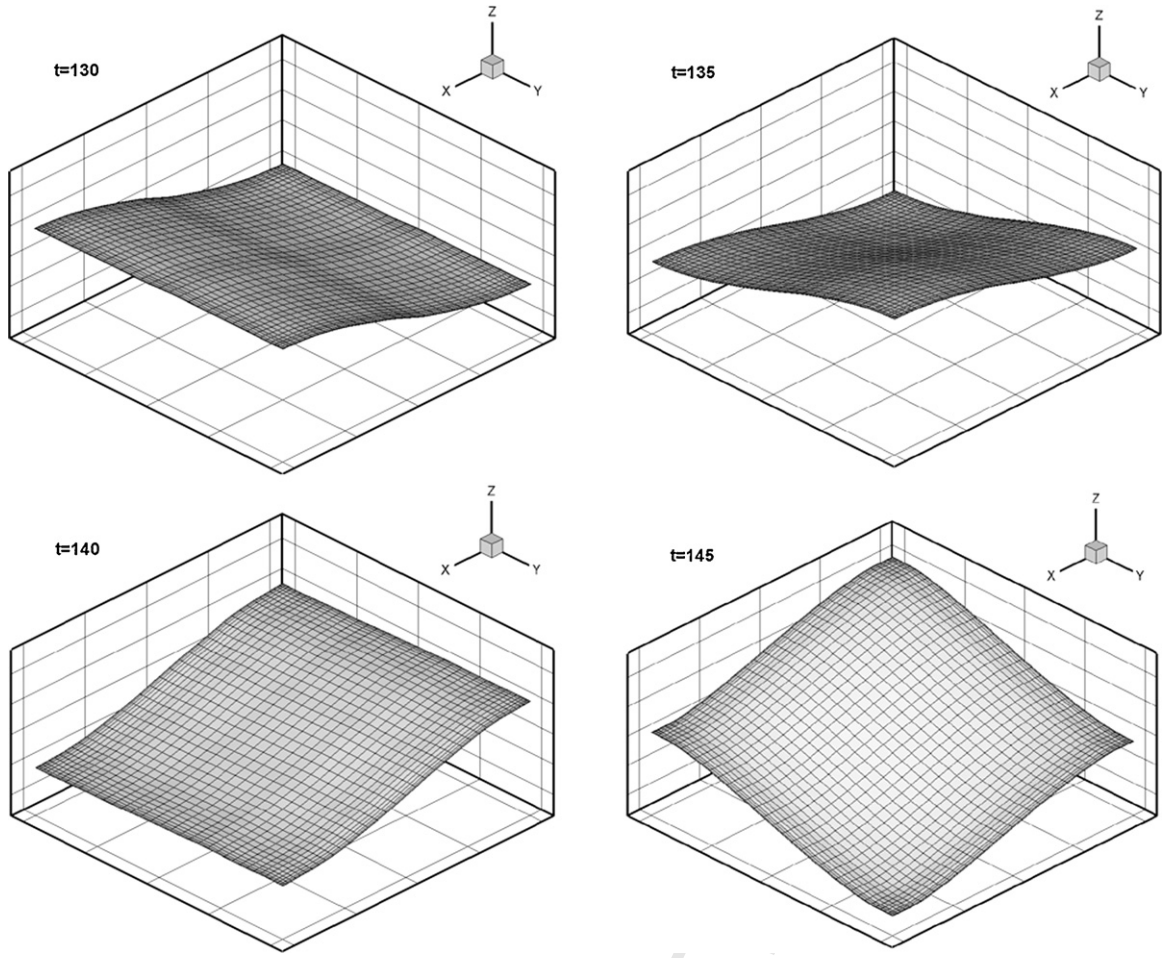

Fig. 9. 3-D visualisations (not to scale) of the liquid free surface sloshing, $A_x/d = 0.001$, $\omega_x = 0.9999\omega_{10}$, $\omega_y = \omega_{20}/2$.

5. Influence of water depth

It is well established that second-order resonant sloshing is dependent on the ratio of still water depth to length of tank. Wu [6] noted that certain occurrences of second-order resonance are valid only for extremely shallow water depths. Using power spectral analysis, Chen and Wu [20] concluded that secondary resonance occurs when $d/a \leq 0.5$. Here, we consider sloshing in a square tank for four different ratios of depth to length ratio: $d/a = 1/1.5$ (deep water), 1/2.5 (finite depth), 1/5 (intermediate depth), and 1/10 (shallow water). The non-dimensional surge excitation amplitude is $A_x/d = 0.001$ and frequency is $\omega_x = \omega_{20}/2$. Figs. 10–13 show the free surface elevation time histories at Point F for all the depth ratios considered.

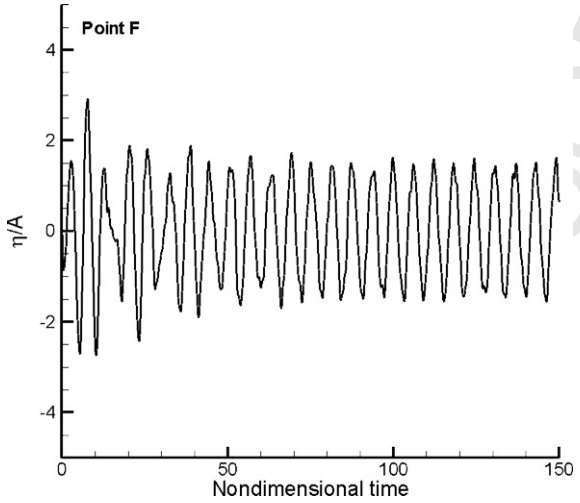

Fig. 10. Free surface elevation time histories at Point F: square tank, $d/a = 1/1.5$, $\omega_x = \omega_{20}/2$, $A_x/d = 0.001$.

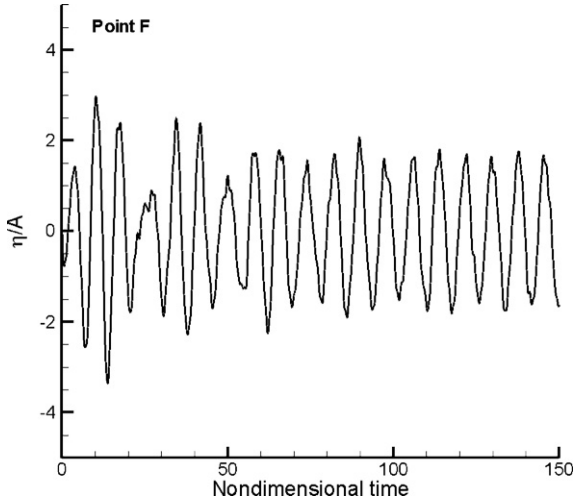

Fig. 11. Free surface elevation time histories at Point F, square tank, $d/a = 1/2.5$, $\omega_x = \omega_{20}/2$, $A_x/d = 0.001$.

Please cite this article in press as: Chern M-J, et al. Fully non-linear simulation of second-order resonance in a three-dimensional tank using the PSME method. Applied Ocean Research (2012), doi:10.1016/j.apor.2012.02.005

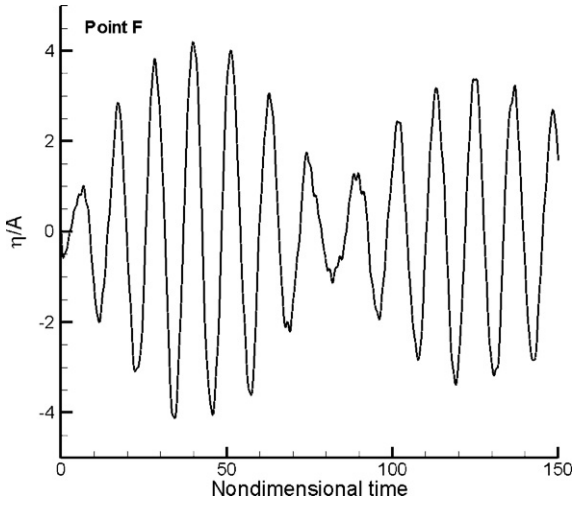

Fig. 12. Free surface elevation time histories at Point F: square tank, $d/a = 1/5$, $\omega_x = \omega_{20}/2$, $A_x/d = 0.001$.

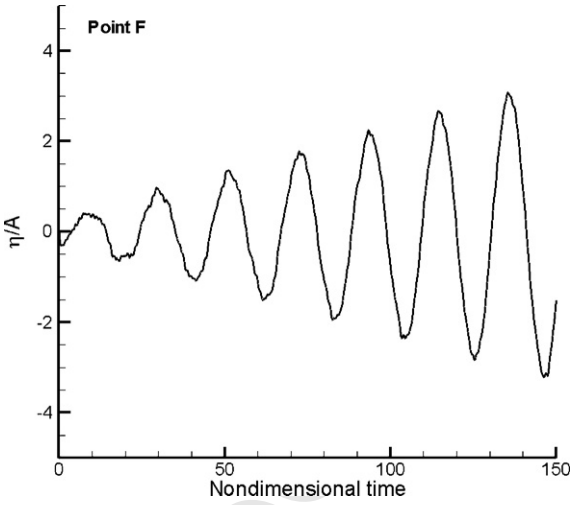

Fig. 13. Free surface elevation time histories at Point F: square tank $d/a = 1/10$, $\omega_x = \omega_{20}/2$, $A_x/d = 0.001$.

The results confirm Chen and Wu's [20] finding that second-order resonance only occurs in shallow water when $\omega_x = \omega_{20}/2$. For $d/a > 0.5$, the wave patterns become more or less periodic after a short transition period. For $d/a = 0.2$, a beating pattern occurs, with an envelope period of about 80 non-dimensional time units. The maximum elevation is more than twice that obtained in the previous cases involving standing waves. Resonance is evident in the shallow water case. As shown in Fig. 4, the pattern becomes standing after a long time, but the elevation is about 50% more than the deep water and the finite depth cases. The wave regime is invariably planar in the x-direction. Fig. 14 depicts the comparison between power spectral densities of all cases.

Changes in excitation frequency can evidently cause the wave pattern to change at various depths. In the shallowest water case, the primary sloshing spectral peak is narrow-banded about the first natural frequency. As the depth increases, the peak becomes broader-band then separates into two distinct peaks (for $d/a > 0.4$) reflecting the difference between the first natural frequency and the forcing frequency. For $d/a > 0.4$, the spectral density of the peak at a frequency half of the second-order natural frequency is substantially larger than that at the first-order natural frequency, and is probably a symptom of non resonant sloshing.

6. Influence of excitation amplitude

Next, we consider the effect of excitation amplitude on second-order resonance in a square tank of dimensions $a/d = b/d = 10$. Five different non-dimensional amplitudes are selected: $A_x/d = 0.001$, 0.005, 0.01, 0.05 and 0.1. The longitudinal excitation frequency is $\omega_x = \omega_{20}/2$. Fig. 15 shows the time histories of free surface elevation at Points E and F for all amplitudes considered. Fig. 16 depicts the corresponding power spectral densities on a logarithmic scale at Point F.

The rate of increase in wave amplitude is almost the same for all values of surge excitation amplitude, except $A_x/d = 0.001$. For $A_x/d = 0.1$, the maximum value of non-dimensional wave elevation

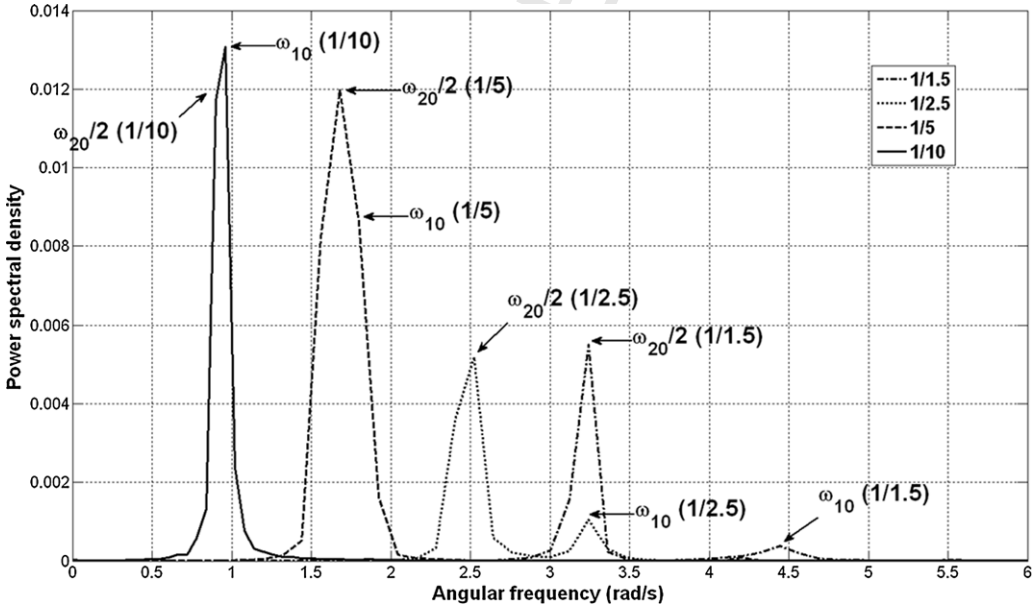

Fig. 14. Power spectral densities for sloshing in a square tank with different depth/length ratios, $A_x/d = 0.001$, $\omega_x = \omega_{20}/2$; $\omega_{10}(1/10) = 0.9683$ rad/s; the response frequencies of interest are $\omega_{20}/2(1/10) = 0.9264$ rad/s; $\omega_{10}(1/5) = 1.8527$ rad/s; $\omega_{20}/2(1/5) = 1.6186$ rad/s; $\omega_{10}(1/2.5) = 3.2373$ rad/s; $\omega_{20}/2(1/5) = 2.4665$ rad/s; $\omega_{10}(1/1.5) = 4.4665$ rad/s; $\omega_{20}/2(1/1.5) = 3.2044$ rad/s.

Please cite this article in press as: Chern M-J, et al. Fully non-linear simulation of second-order resonance in a three-dimensional tank using the PSME method. Applied Ocean Research (2012), doi:10.1016/j.apor.2012.02.005

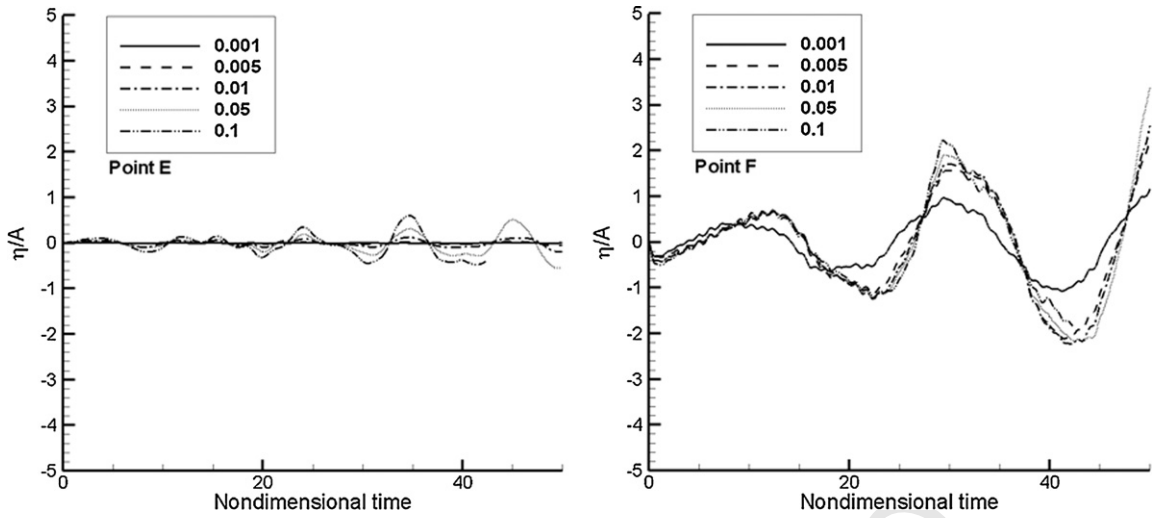

Fig. 15. Free surface elevation time histories for different surge excitation amplitudes at a frequency $\omega_x = \omega_{20}/2$.

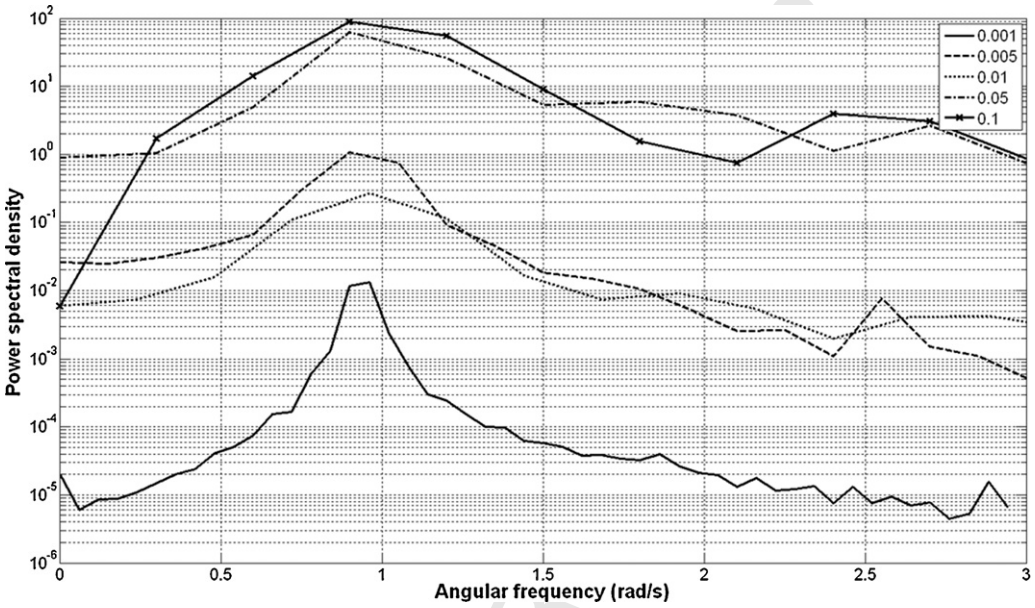

Fig. 16. Power spectral densities for different surge excitation amplitudes at a frequency $\omega_x = \omega_{20}/2$.

η/A exceeds 2.0 after about a non-dimensional time of about 40 units. At Point E, the wave steepens due to non-linearity at the largest excitation amplitude, and a bore eventually develops. Fig. 17 presents a snapshot of the water surface obtained at non-dimensional time $t = 41.2$ units for an excitation amplitude $A_x/d = 0.1$. At Point F, a steep wave of large amplitude has developed. The overall sloshing motion is planar and the wave pattern is resonant in all cases. Also, some oscillatory components can be seen in all cases especially in the first and second cycles which are like three-dimensional sloshing models perturbations [11]. Dominant resonant sloshing frequencies in all cases occur at the first natural frequency and half of the second natural frequency. However, it should be noted that the influence of the forcing excitation frequency ($\omega_{20}/2$) increases slightly with increasing excitation amplitude.

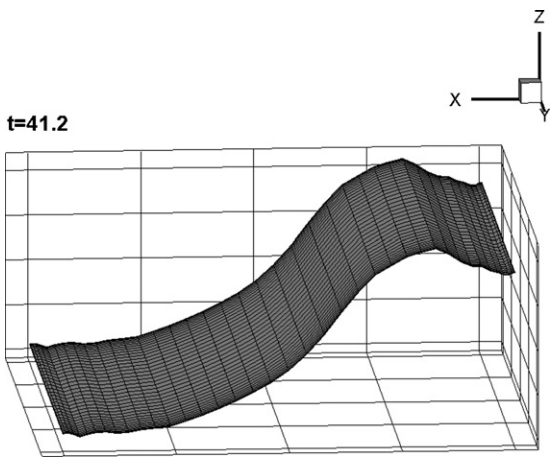

Fig. 17. 3D visualisation (not to scale) of the free surface for $A_x/d = 0.1$, $\omega_x = \omega_{20}/2$.

7. Influence of base aspect ratio

The final part of the parameter study examines the effect of the ratio of width to length of the base of the tank on its sloshing

Please cite this article in press as: Chern M-J, et al. Fully non-linear simulation of second-order resonance in a three-dimensional tank using the PSME method. Applied Ocean Research (2012), doi:10.1016/j.apor.2012.02.005

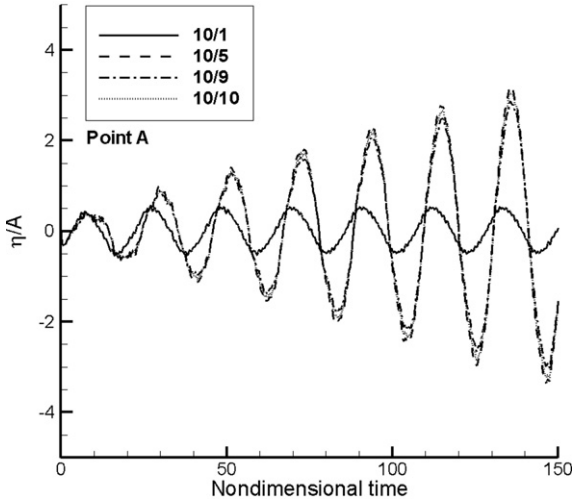

Fig. 18. Free surface elevation time histories for different base aspect ratios: surge excitation at frequency $\omega_x = \omega_{20}/2$.

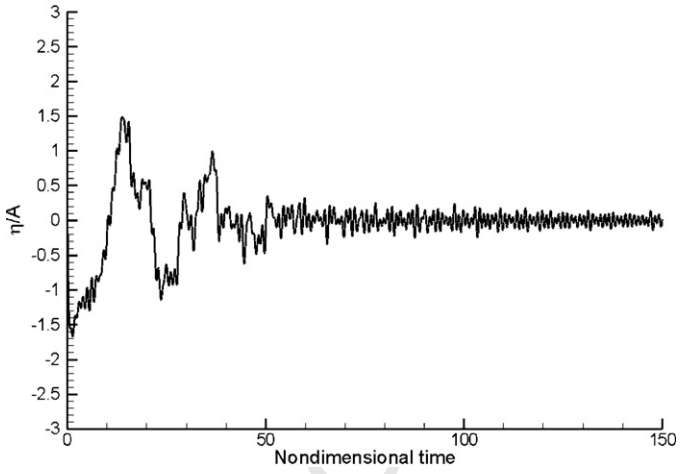

Fig. 20. Free surface time history at Point A for heave excitation frequency $\omega_z = 0.9999\omega_{20}$.

properties. It should of course be mentioned that there has been substantial research on first-order sloshing in tanks of varying base aspect ratio (see e.g. [21,22,13]). Here, we consider shallow water sloshing ($d/a = 0.1$) in tanks with base aspect ratios, $a/b = 10/1$ (very long base), 10/5 (half wide base), 10/9 (nearly square base) and 10/10 (square base). The excitation is in the longitudinal direction with non-dimensional amplitude $A_x/d = 0.001$ and frequency $\omega_x = \omega_{20}/2$.

Fig. 18 compares the free surface elevation time histories at Point A for the various base aspect ratios. Standing waves tend to evolve rapidly when the basin is far from square. Resonance occurs with the free surface elevation growing at a similar rate when the basin is square or nearly square. In all cases, the wave regime is planar. Fig. 19 depicts the corresponding power spectra using a logarithmic scale. The first harmonic sloshing mode invariably occurs at the first natural frequency. The influence of the forcing frequency increases as the tank width increases. As for the free surface elevation time histories, the power densities are very close for $a/b > 1$.

8. Vertical excitation

In this section the forced sloshing of liquid in a 3D tank subjected to vertical motion (heave) is concerned. The waves generated by the vertical tank motion are called Faraday waves. A considerable number of papers have been published on this topic, which have been reviewed by Jiang et al. [23]. Here we consider the vertical excitation of water in a tank of dimensions $a/d = b/d = 10$ and the non-dimensional amplitude is $A_z/d = 0.001$. Figs. 20–23 show the free surface elevation time histories obtained at Point A for excitation frequencies equal to $0.9999\omega_{20}$, $\omega_{20}/2$, $\omega_{20} + \omega_{10}$ and $\omega_{20} - \omega_{10}$. It should be noted that a small initial perturbation of the horizontal velocities is chosen as the initial condition. Values of $\frac{dD_x}{dt}\Big|_{t=0}$ and $\frac{dD_y}{dt}\Big|_{t=0}$ in Eq. (9) are set to the value of the excitation frequency in each case and set to zero when $t \neq 0$ [4]. In all cases, the waves are irregular and decay gradually. These results are expected, because the values of excitation frequencies are almost small due to the large base. Therefore, the resonance or the violent free-surface motion conditions do not occur.

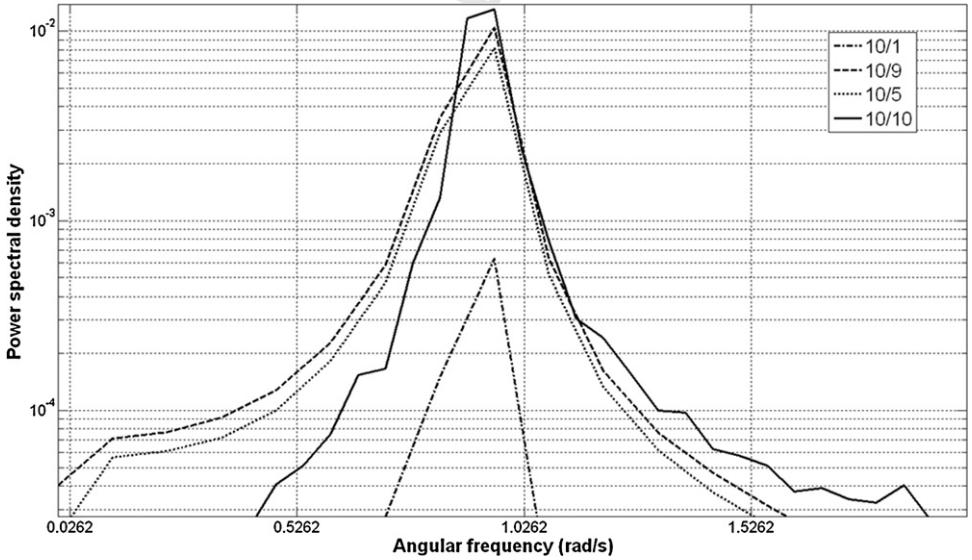

Fig. 19. Power spectral densities for different base aspect ratios: surge excitation at frequency $\omega_x = \omega_{20}/2$.

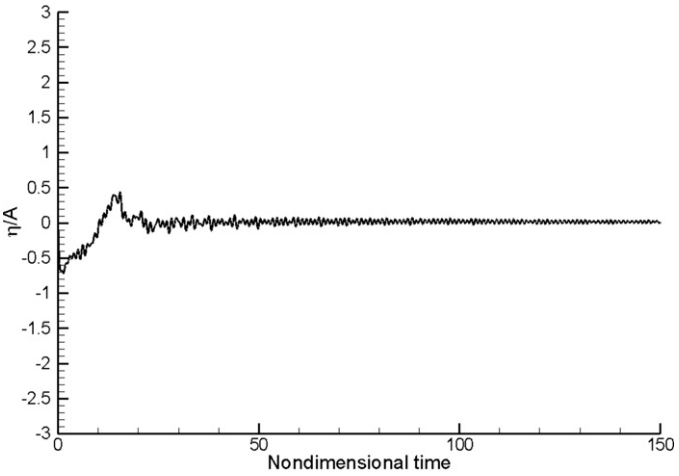

Fig. 21. Free surface time history at Point A for heave excitation frequency $\omega_z = \omega_{10}/2$.

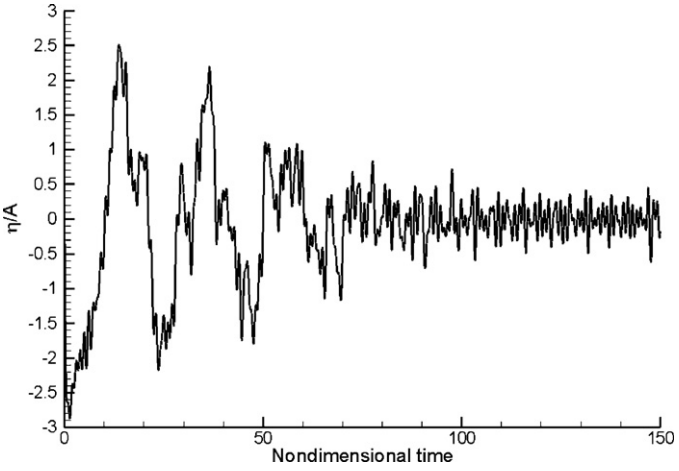

Fig. 22. Free surface time history at Point A for heave excitation frequency $\omega_z = \omega_{20}/\omega_{10}$.

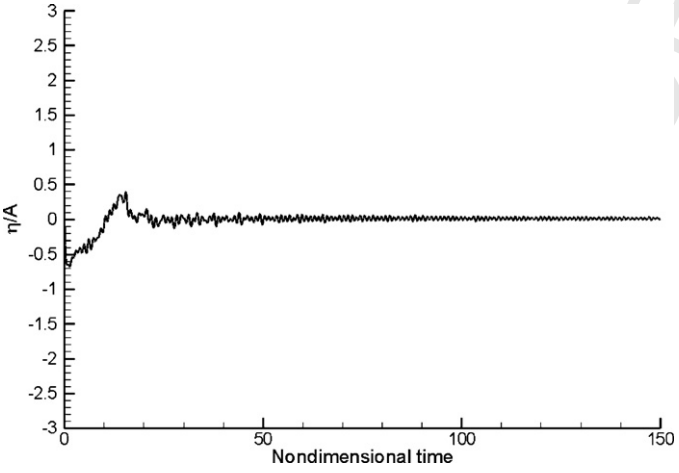

Fig. 23. Free surface time history at Point A for heave excitation frequency $\omega_z = \omega_{20} - \omega_{10}$.

9. Conclusions

A validated pseudospectral σ-transformation model has been used to simulate second-order resonance shallow water waves in a 3D rectangular tank, where the still water depth to length ratio is $d/a = 0.1$. Several important conditions observed by Wu [6] are considered. The results show that large-amplitude sloshing motions occur, but can have a beating pattern due to the effect of wave nonlinearity. Moreover, second-order resonance in shallow water can entirely change the wave motion to a mode at the first natural frequency. A parameter study has been undertaken to investigate the effects of altering the water depth, the base aspect ratio, and the excitation amplitude on the wave regime and the wave pattern. The reference value of non-dimensional amplitude A/d was 0.001. In studying the effect of water depth, results were presented for cases where sloshing was driven by surge excitation at a forcing frequency equal to half the second-order natural frequency. Under these conditions, resonance occurs only in shallow water for $d/a < 0.5$. From the power spectra, it appears that this phenomenon may be due to the increasing difference between the first natural frequency and the forcing frequency. The intensities of the free surface motion harmonics decrease as the ratio of depth to length increases. It is found that the wave regimes and patterns hardly change and the dominant free surface motion frequencies remain almost the same with excitation amplitude for second-order resonant sloshing in shallow water. Due to their non-linearity, the largest amplitude waves become progressively steep until a bore is created. In examining the effect of base aspect ratio, surge excitations were imposed at a frequency half that of the second natural frequency. It is found that the sloshing motions alters from a standing wave pattern to resonant oscillations the more square the tank. Finally, the excitation in the vertical direction with the same frequencies and conditions of Section 4 was considered. The decay patterns were observed in all cases.

Acknowledgments

The authors are grateful to the National Science Council of Taiwan for its generous financial support (NSC 99-2221-E-011-041). The first author would also like to express gratitude for his Taiwan Scholarship from the National Science Council of Taiwan. Furthermore, the helpful comments of the reviewers and the editor are greatly appreciated.

References

[1] Ibrahim RA. Liquid sloshing dynamics. Cambridge, UK: Cambridge University Press; 2005.
[2] Faltinsen OM, Timokha AN. Sloshing. Cambridge, UK: Cambridge University Press; 2009.
[3] Faltinsen OM. A numerical nonlinear method of sloshing in tanks with two-dimensional flow. J Ship Res 1978;22:193–202.
[4] Wu GX, Ma QW, Eatock Taylor R. Numerical simulation of sloshing waves in a 3d tank based on a finite element methods. Appl Ocean Res 1998;20:337–55.
[5] Chern MJ, Borthwick AGL, Eatock Taylor R. A pseudospectral (σ-transformation model of 2D nonlinear waves. J Fluid Struct 1999;13:607–30.
[6] Wu GX. Second-order resonance of sloshing in a tank. Ocean Eng 2007;34:2345–9.
[7] Wang CZ, Wu GX. Analysis of second-order resonance in wave interactions with floating bodies through a finite-element method. Ocean Eng 2008;35:717–26.
[8] Wang CZ, Wu GX, Khoo BC. Fully nonlinear simulation of resonant motion of liquid confined between floating structures. Comput Fluid 2011;44:89–101.
[9] Liu YL, Yue DKP, Kim MH. First- and second-order responses of a floating toroidal structure in long-crested irregular seas. Appl Ocean Res 1993;15:155–67.
[10] Firouz-Abadi RD, Ghasemi M, Haddadpour H. A modal approach to second-order analysis of sloshing using boundary element method. Ocean Eng 2011;38:11–21.
[11] Faltinsen OM, Rognebakke OF, Timokha AN. Resonant three-dimensional nonlinear sloshing in a square-base basin. J Fluid Mech 2003;487:1–42.

Please cite this article in press as: Chern M-J, et al. Fully non-linear simulation of second-order resonance in a three-dimensional tank using the PSME method. Applied Ocean Research (2012), doi:10.1016/j.apor.2012.02.005

[12] Faltinsen OM, Rognebakke OF, Timokha AN. Classification of three-dimensional nonlinear sloshing in a square-base tank with finite depth. J Fluid Struct 2005;20:81–103.
[13] Faltinsen OM, Rognebakke OF, Timokha AN. Resonant three-dimensional nonlinear sloshing in a square-base basin. Part 3. Base ratio perturbations. J Fluid Mech 2006;551:93–116.
[14] Ku HC, Hatziavramidis D. Solutions of the 2-dimensional Navier–Stocks equations by Chebyshev expansion methods. Comput Fluid 1985;13:99–113.
[15] Chern MJ, Borthwick AGL, Eatock Taylor R. Simulation of non-linear free surface motions in a cylindrical domain using a Chebyshev Fourier spectral collocation method. Int J Numer Methods Fluids 2001;36:465–96.
[16] Vaziri N, Chern MJ, Borthwick AGL. Pseudospectral σ-transformation model of solitary waves in a tank with uneven bed. J Comput Fluid 2011;49:197–202.
[17] Dean RG, Dalrymple RA. Water waves mechanics. World Scientific Press; 2000.
[18] Philips NA. A coordinate system having some special advantages for numerical forecasting. J Appl Meteorol 1957;14:184–5.
[19] Chern MJ, Vaziri N, Syamsuri S, Borthwick AGL. Pseudospectral solution for three-dimensional non-linear sloshing in shallow water rectangular tank. J Fluid Struct, in press. Q3
[20] Chen BF, Wu CH. Effects of excitation angle and coupled heave–surge–sway motion on fluid sloshing in a three-dimensional tank. J Mar Sci Technol 2011;16:22–50.
[21] Feng ZC, Sethna PR. Symmetry-breaking bifurcations in resonant surface waves. J Fluid Mech 1993;199:495–518.
[22] Ockendon H, Ockendon JR, Peake MR, Chester W. Geometrical effects in resonant gas oscillations. J Fluid Mech 1993;257:201–17.
[23] Jiang L, Ting CL, Perlin M, Schultz W. Moderate and steep Faraday waves: instabilities, modulations and temporal asymmetries. J Fluid Mech 1996;329:275–307.

Please cite this article in press as: Chern M-J, et al. Fully non-linear simulation of second-order resonance in a three-dimensional tank using the PSME method. Applied Ocean Research (2012), doi:10.1016/j.apor.2012.02.005